Pergamon

PII: S0306-4549(96)00013-8

Ann. Nucl. Energy, Vol. 24, No. 2, pp. 79–98, 1997
Published by Elsevier Science Ltd
Printed in Great Britain
0306-4549/97 $15.00 + 0.00

VALIDATION OF THE MONTE CARLO CODE MCNP-DSP

T. E. VALENTINE and J. T. MIHALCZO

Oak Ridge National Laboratory†, P.O. Box 2008, Oak Ridge, TN 37831-6004, USA

(Received 5 February 1996)

Abstract—Several calculations were performed to validate MCNP-DSP, which is a Monte Carlo code that calculates all the time and frequency analysis parameters associated with the ^{252}Cf-source-driven time and frequency analysis method. The frequency analysis parameters are obtained in two ways: directly by Fourier transforming the detector responses and indirectly by taking the Fourier transform of the autocorrelation and cross-correlation functions. The direct and indirect Fourier processing methods were shown to produce the same frequency spectra and convergence, thus verifying the way to obtain the frequency analysis parameters from the time sequences of detector pulses MCNP-DSP was verified by calculations of configurations of sources and detectors with accurately known theoretical answers. The calculated value of the ratio of spectral densities, $R(\omega)$, was shown to be independent of detection efficiency and in some cases source intensity as theoretically predicted. The neutron and gamma ray time distributions after ^{252}Cf fission from MCNP-DSP for simple configurations of source and detectors in air and with a small sample of beryllium between the source and detector were compared with measurements. In addition, calculations were performed for measurements using the ^{252}Cf-source-driven noise analysis technique. MCNP-DSP adequately calculated the measured low-frequency values of $R(\omega)$ from the detector responses due to neutrons and gamma rays for the unmoderated, unreflected uranium metal cylinders using the ENDF/B-IV cross-sections. These calculations also showed that the frequency dependence of the spectra obtained from the netron detector and from the gamma-ray detector responses, in this case, is the same. The ability to calculate the measured low-frequency value of $R(\omega)$ for two tightly coupled uranium metal cylinders separated by a borated plaster disk, using detectors sensitive only to gamma rays, further demonstrated that the code could accurately calculate the detector response due to gamma rays. The results of the calculations were shown to be strongly dependent on the cross-section data sets used in the analysis. The calculated frequency analysis parameters changed significantly when using different cross-section data sets, although the neutron multiplication factor k changed slightly. This demonstrated the

†Managed by Lockheed Martin Energy Research Corp. for the U.S. Department of Energy under contract DE-AC05-96OR22464.

known increased sensitivity in calculating the noise-measured parameters rather than calculating k when validating computational methods and cross-section data. This more general neutron and gamma-ray treatment provides the most comprehensive calculation of the measured parameters from a ^{252}Cf-source-driven time and frequency analysis measurement and is useful for planning experiments, analyzing the results of measurements, and verifying Monte Carlo neutron and gamma-ray transport methods. MCNP-DSP can be used in the planning and analysis of measurements by the source-driven time and frequency analysis method for nuclear weapons and/or component identification, subcriticality measurements, nuclear material control and accountability, process monitoring and control, and quality assurance of fissile components, such as reactor fuel elements. In addition, it can be used to obtain the calculational bias in the calculation of the neutron multiplication factor from subcritical experiments, a quantity that is essential to the criticality safety specialist for criticality safety assessments. This general Monte Carlo model eliminates the need for the limited point kinetics models for interpreting subcriticality measurements by this method. Published by Elsevier Science Ltd

1. INTRODUCTION

The Monte Carlo code MCNP-DSP (Valentine and Mihalczo, 1996) was developed to calculate time and frequency signatures of the ^{252}Cf-source-driven noise analysis measurement (Mihalczo, 1970; Mihalczo, 1971; Paré and Mihalczo, 1975). This measurement method employs two or more particle detectors along with a ^{252}Cf source to characterize or to determine the reactivity of a subcritical assembly. The source, which is contained within an ionization chamber, is placed in or near the subcritical fissile configuration to initiate the fission chain multiplication process. For each spontaneous fission of ^{252}Cf, an electrical pulse is produced that indicates the time of fission and emission of neutrons and gamma rays. The particle detectors are placed in or near the fissile assembly to measure particles from the fission chains induced by the spontaneous fission of the ^{252}Cf source. A certain ratio of spectral densities, $R(\omega)$, obtained from the measured data is independent of detection efficiency and sometimes source intensity. The ratio of spectral densities is defined as

$$R(\omega) = \frac{G_{12}^{*}(\omega)\, G_{13}(\omega)}{G_{11}(\omega)\, G_{23}(\omega)} \tag{1.1}$$

where ω is the angular frequency; G_{12}^{*} is the complex conjugate of the cross-power spectral density (CPSD) of the source detector #1 and detector #2, which detects particles from fission; G_{13} is the CPSD of the source detector #1 and the particle detector #3; G_{11} is the auto-power spectral density (APSD) of the source detector; and G_{23} is the CPSD between the two particle detectors. This article presents comparisons of the measured and calculated time distributions of particle counts in a detector after ^{252}Cf fission. A comparison of theoretically known or measured frequency analysis parameters, in particular the ratio of spectral densities, with those calculated by MCNP-DSP is used for validation.

2. VALIDATING MCNP-DSP

2.1. Computer code validation

The principal means of validating computer codes is by direct calculation of measured observables or by calculating parameters that have a precise value known from accepted theoretical models. Several calculations were performed to validate the calculation of the neutron emission spectra and gamma ray emission from the spontaneous fission of ^{252}Cf, the detection process, the timing of the detection process, and the time and frequency response calculations. An alternative independent way of obtaining the frequency response from the detector responses confirms the frequency response calculations. Calculations were also performed to validate certain known properties of the ratio of spectral densities.

2.2. Energy spectra and detection process validation

The validation of the neutron energy spectrum and gamma-ray emission and the validation of the detection process were performed by calculations with the source separated from a detector in air and comparing the results with experiment. The time distribution of neutron counts in the detector after the spontaneous fission of ^{252}Cf with the source and detector separated in air is directly related to the neutron energy spectra from fission. Experimentally, measurement of the time distribution of neutron counts after ^{252}Cf fission is used to verify that the detection equipment is functioning properly. A measurement and a calculation were performed with the source placed 1105 mm away from the detector in air. The detector used in these measurements and in calculations was a proton-recoil, liquid, organic scintillator (Bicron 501) of 114.3-mm OD and 57.2 mm thick. In the calculation and the measurement, the neutron threshold was set to 0.8 MeV, and the gamma-ray threshold was set to 0.1 MeV. Figure 1 compares the measured and calculated neutron responses as a function of time after ^{252}Cf fission. The calculated neutron response in counts per ^{252}Cf fission per Δt is in excellent agreement with the measured response expressed in the same units. If the neutron energy spectrum from fission used in this calculation is a good representation of the measured spectrum, this result indicates that the neutron detection process is adequately represented. In the measurements, the detector efficiency curve rolls off to zero around 0.5 MeV. The neutron threshold is defined experimentally as the neutron energy at which the efficiency is half its maximum value. This allows for a small number of low-energy neutrons to be detected; therefore, there will be a slight difference between the measured and calculated response at the longer times. This is evident in Fig. 1 around 100 ns. The measured and calculated gamma-ray responses are shown in Fig. 2. Since the calculated gamma-ray response does not suffer from the time resolution that occurs in these measurements, the gamma-ray peak obtained from the calculation is much narrower than that obtained in the measurement, as is evident in Fig. 2. The timing uncertainty in the measured response is due to the uncertainties in the measurement of the time of ^{252}Cf fission and the time of detection, which depends on time resolution and size of the detector. Nevertheless, the area under the curves should be equivalent. The areas under the measured and calculated curves agree to within 5%, thus validating the gamma-ray detection process to this accuracy. Because all gamma rays travel at the speed of light, the time of arrival of the gamma

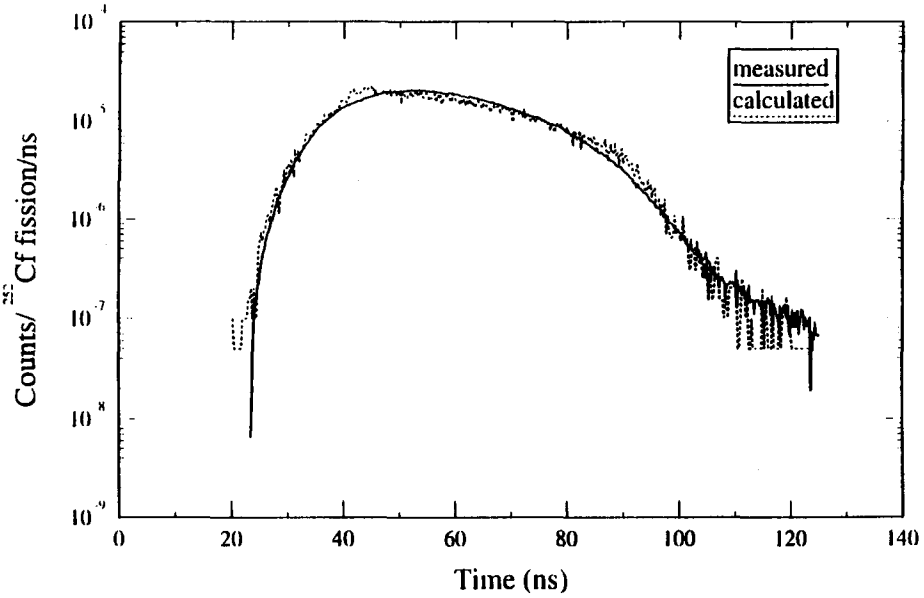

Fig. 1. Calculated and measured neutron response as a function of time after ^{252}Cf fission for source and detector separated by 1 m in air.

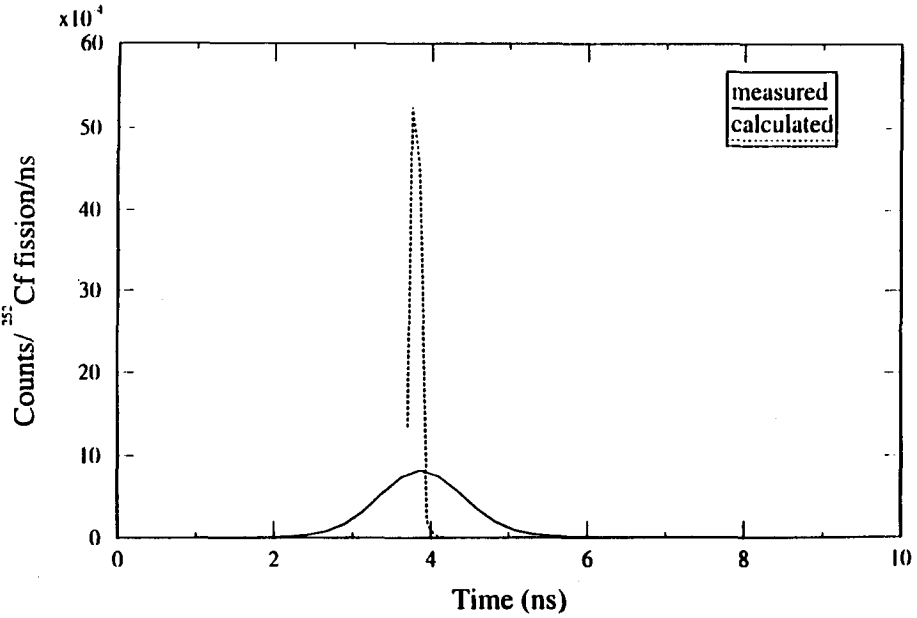

Fig. 2. Calculated and measured gamma ray response as a function of time after ^{252}Cf fission for source and detector separated by 1 m in air.

rays at the front face of the detector is known precisely. For the given source–detector configuration, the time of arrival of the gamma rays is 3.72 ns at the front face of the detector; consequently, this time corresponds to the gamma-ray peak in the calculation.

The calculated peak has some width because the thickness of the detector adds some dispersion to the calculated peak. From these comparisons, it is evident that if the neutron emission and gamma-ray emission spectra are good representations of the actual spectra the particle detection process for this type of detector is adequately represented, thus confirming the simplifying assumptions made for this type of scattering detector.

2.3. Time response validation with attenuating media

To accurately calculate the detector responses from particles traveling through an attenuating medium, the time of detection needs to be calculated precisely. To test the determination of time in the calculation and the sorting of detector pulses when material is placed between the source and the detector, a calculation was performed with a 36.3-mm thick piece of beryllium metal placed between the source and the plastic scintillator, as shown in Fig. 3. Beryllium metal was used because the total cross-section of beryllium is well known and has a well-characterized resonance at 2.78 MeV. The total cross-section has been measured using a similar source and detector configuration (Mihalczo and Hill, 1971). The detector response in counts per ^{252}Cf fission per Δt is shown in Fig. 4. The depression in the detector response near 44 ns corresponds to the resonance in the total cross-section at 2.78 MeV. This is verified by calculating the time it takes for 2.78 MeV neutrons to travel to the center of the detector.

2.4. Frequency response test

To validate the computation of the frequency spectra, the Fourier processing routines had to be validated. A simple procedure to test the processing routines is to perform a noise calculation with the ^{252}Cf source placed between the detectors. This test is frequently used to ensure that the measurement system is working properly. The ratio of spectral densities, $R(\omega)$, has a well-defined value for this particular source–detector configuration. The measured ratio of spectral densities is theoretically equal to the inverse of the Diven factor for the ^{252}Cf source if all of the ^{252}Cf neutrons are detected. The Diven factor for the ^{252}Cf source from Spencer's data is equal to 0.846 (Spencer *et al.*, 1982). This results in the ratio of spectral densities being equal to 1.18 at all frequencies.

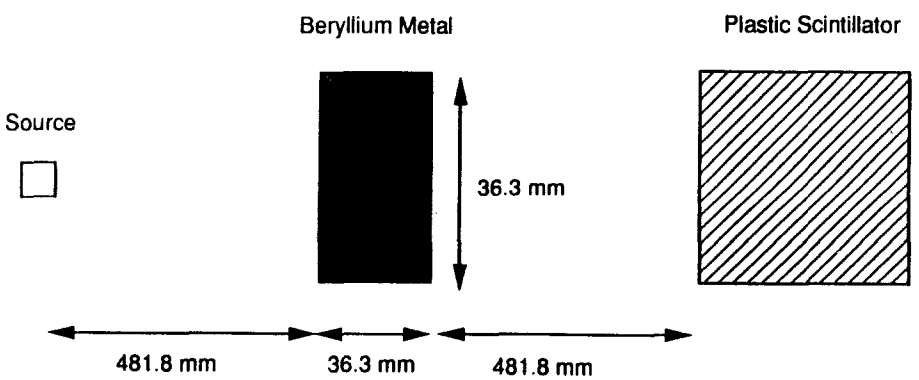

Fig. 3. Sketch of source-detector model for beryllium tranmission calculation (not to scale).

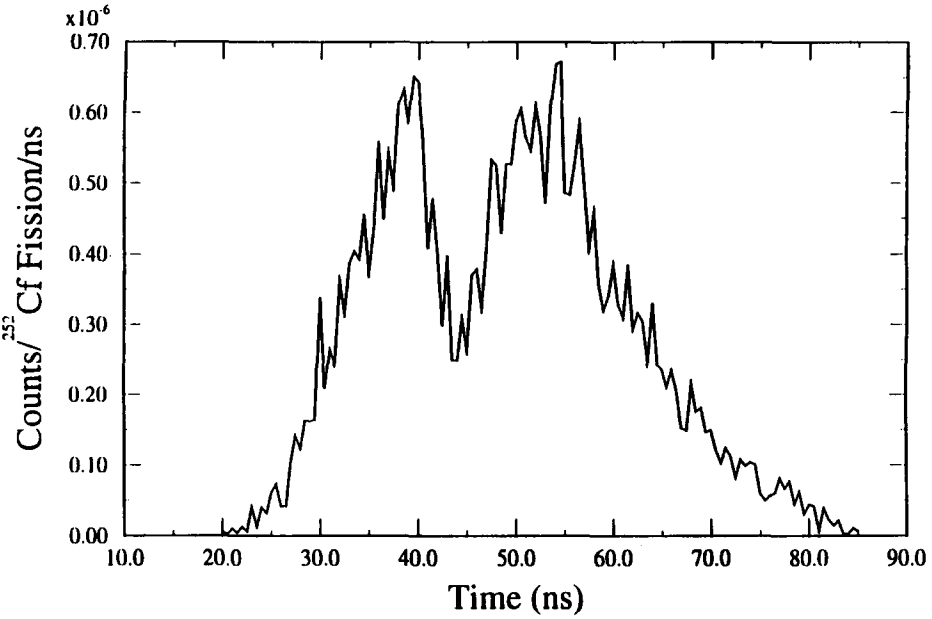

Fig. 4. Calculated correlated neutron time distribution after ^{252}Cf fission for beryllium metal cylinder.

The detectors used in this calculational model were ^{3}He detectors in which the gas pressure was artificially high (3000 atm), so that all neutrons from the source were detected. For this particular source–detector configuration, the calculated value of the ratio of spectral densities from MCNP-DSP is 1.181 ± 0.001 using these highly absorbing neutron detectors. A similar calculation was performed for the gamma rays. The theoretical value of the ratio of spectral densities for the gamma rays is 0.966, obtained from the inverse of a Diven-like factor obtained from Brunson's measurements of the multiplicity for gamma-ray emission from ^{252}Cf (Brunson, 1982). A calculation was performed placing the source between two large pieces of lead that were treated as the detectors. The calculated value of the ratio of spectral densities is 0.956 ± 0.002. The 1% difference between the theoretical and the calculated value is attributed to gamma rays that scatter between detectors, thus increasing the coherence between detectors and slightly reducing the ratio of spectral densities. These tests indicate that the Fourier processing routines, which obtain the spectra by directly Fourier transforming the blocks of detector time responses, are correct.

2.5. Direct or indirect frequency analysis calculations

Because there are theoretically two independent ways to process the detector signals to obtain the APSDs and CPSDs, both methods for processing the detector time responses should produce the same results. The frequency spectra can be obtained directly by Fourier transforming the detector response and performing the complex multiplication, or indirectly by Fourier transforming the autocorrelations and cross-correlations of the detector responses. To perform this analysis for various values of the coherence, a 108.17-mm high uranium metal cylinder with a 177.71-mm diameter was analyzed with

detectors of varying size. The coherence (γ_{ij}^2) is defined as the ratio of the squared magnitude of the CPSD between two signals divided by the product of the APSDs of the two signals. By varying the detector diameter, the coherences between the detectors will change. The uranium metal had a density of 18.76 g/cm^3 and consisted of 93.15 wt% ^{235}U, 5.64 wt% ^{238}U, 0.97 wt% ^{234}U, and 0.24 wt% ^{236}U. The detectors used in the calculation are plastic scintillators surrounded by a 6.35-mm thick lead cup. The detectors were symmetrically positioned adjacent to the radial surface at the midplane, while the source was located on top of the cylinder on the centerline. This configuration is shown in Fig. 5. A comparison of the low-frequency values of the coherences obtained from both methods is presented in Table 1. As can be seen from these results, the low-frequency values of the coherences are independent of the way in which the data were processed. Thus the ratio of spectral densities that can be obtained from the coherences does not depend on the way in which the data are processed. These quantities are obtained from the APSDs and CPSDs, which did not vary either. The error of the coherence functions for the two methods is the same for the same number of data blocks. This means that the indirect method will produce data as accurately as direct Fourier processing. The agreement of the results from the two independent methods confirms the calculation of the frequency-dependent functions from the blocks of data. Figure 6 contains a comparison of the coherence between the source and detectors obtained by directly Fourier transforming the detector signals and that obtained by Fourier transforming the cross-correlation

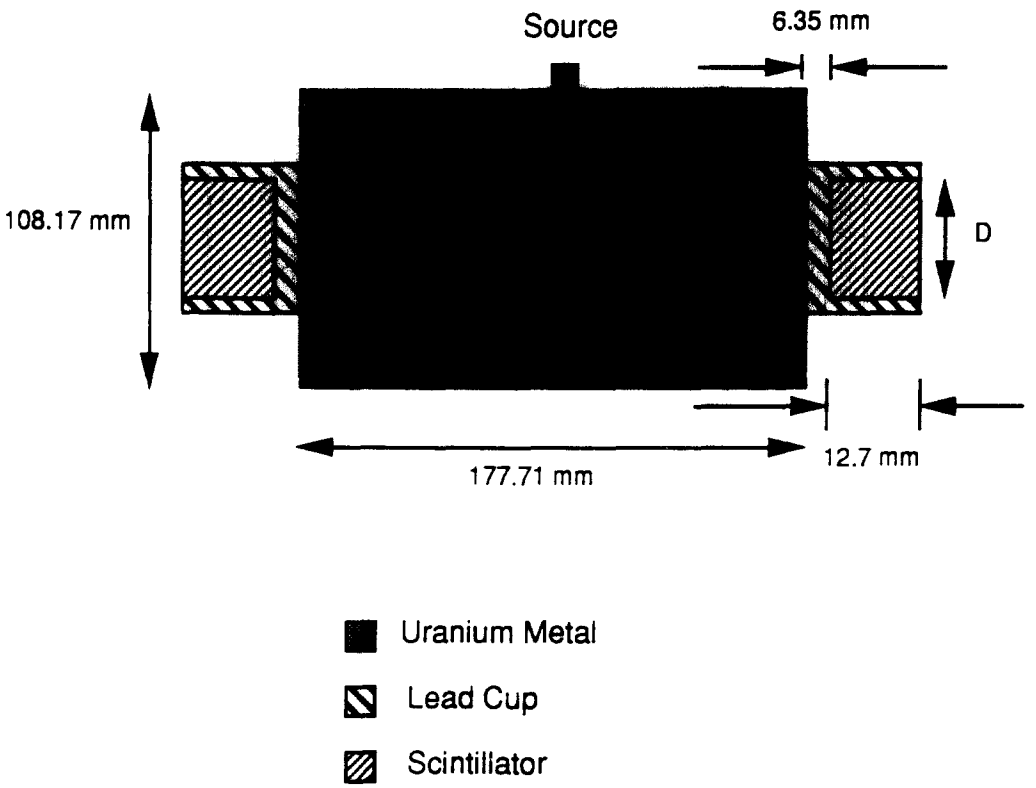

Fig. 5. Sketch of source–detector configuration for the 108.17-mm-high uranium metal cylinder.

Table 1. Low-frequency values of calculated coherences obtained by direct and indirect Fourier processing of detector responses†

Detector diameter‡ (mm)	Number of data blocks	γ_{12}^2	γ_{23}^2
50.8	5000	0.0174 ± 0.0007	0.137 ± 0.002
		(0.0174 ± 0.0007)	(0.137 ± 0.002)
25.4	25000	0.00641 ± 0.00016	0.0130 ± 0.0021
		(0.00649 ± 0.00016)	(0.0131 ± 0.0021)
10.37	200000	0.00110 ± 0.00002	0.00039 ± 0.000011
		(0.00110 ± 0.00002)	(0.00039 ± 0.000009)
4.234	200000	0.000189 ± 0.000007	0.0000114 ± 0.0000006
		(0.000190 ± 0.000010)	(0.0000114 ± 0.0000006)

†Values in parentheses are from calculations using Fourier transforms of correlation function. Other values are for direct Fourier processing of data block. All values are averages up to 100 kHz.
‡Detector diameter varied to produce changes in coherence.

function for a detector diameter of 10.37 mm. Figure 7 is a similar comparison for the coherence between both detectors. As can be seen in Figs 6 and 7, there is no statistically significant difference between the two methods of processing the data. The values in Figs 6 and 7 are not identical because different random numbers were used for each calculation that resulted in the time sequences of pulses at the detectors being different.

2.6. Analysis of ratio of spectral densities

Certain known properties of the ratio of spectral densities confirmed by measurements and simple theory allow for additional validation of the calculational procedure. The low-frequency value of the ratio of spectral densities can be dependent in some special cases on the placement of the detectors. To show that the ratio of spectral densities is affected by the location of the detectors, calculations were performed with detectors spaced 200 mm from the source at 90° angles to each other in a vacuum and also at 180° to each other. This spacing was chosen to have a small solid angle and to ensure that no significant scattering of particles from one detector into another occurred. Table 2 contains a comparison of the ratio of spectral densities for detectors positioned at 90° and 180° from each other. The results show that the ratio of spectral densities is affected by the position of the detectors because of the angular distribution of neutrons from the spontaneous fission of ^{252}Cf. For detectors 180° apart, the probability of a count in the second detector after a count in the first detector is enhanced because of the angular distribution data, since the angular distribution data have a strong back–forward asymmetry. This results in an increase in the value of γ_{23}^2 and a decrease in the ratio of spectral densities.

The low frequency value of the ratio of spectral densities is independent of the detector efficiency and of source strength for fissile systems with no significant additional sources to produce detected events. To test the expected insensitivity of the ratio of spectral densities to the source strength and the detector efficiency, several calculations were performed for the 292-mm high uranyl nitrate solution in a 251-mm ID cylindrical tank. A detailed description of this geometry can be found elsewhere (Mihalczo *et al.*, 1990). This system was selected because the detection efficiency could be changed by changing the detector

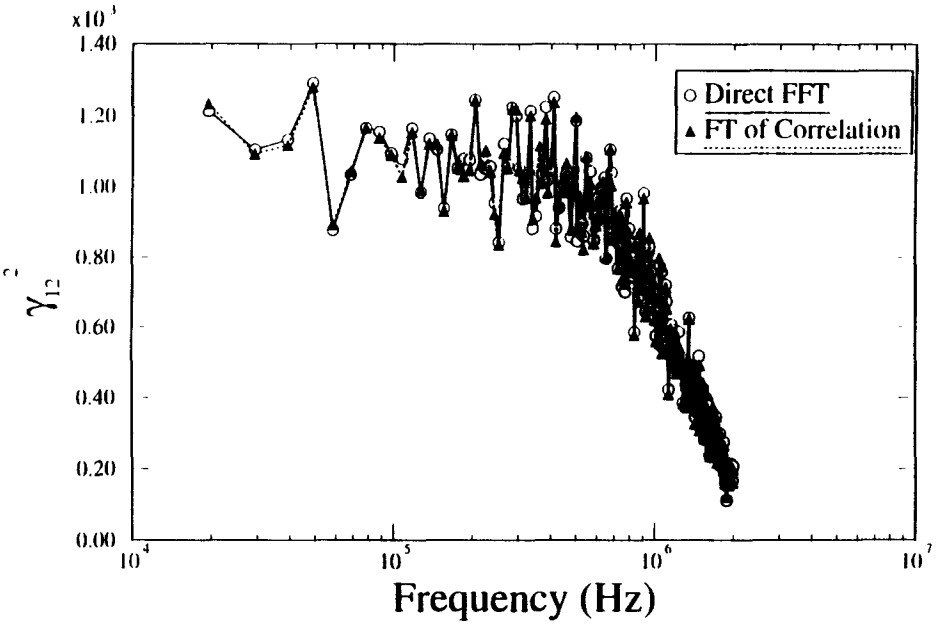

Fig. 6. Comparison of γ^2_{12} between the direct Fast Fourier Transform (FFT) of the detector response and the Fourier Transform of the correlation function for a 17.771-cm-diam uranium metal cylinder with a 10.37-mm-diam detector.

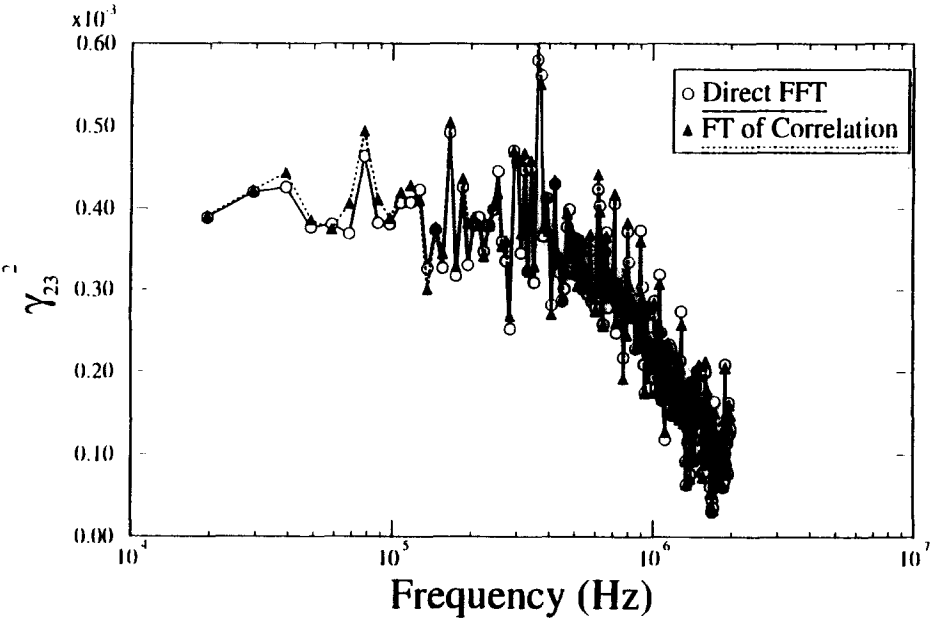

Fig. 7. Comparison of γ^2_{23} between direct FFT of the detector response and the Fourier Transform of the correlation function for a 17.771-cm-diam uranium metal cylinder with 10.37-mm-diam detectors.

Table. 2. Angular distribution effects on ratio of spectral densities for source and detectors in a vacuum†

Angle (degrees)	Number of data blocks	γ_{12}^2‡ ($\times 10^{-3}$)	γ_{23}^2§ ($\times 10^{-4}$)	$R(\omega)$
90	1 200 000	8.98 ± 0.02	0.213 ± 0.009	1.93 ± 0.005
180	1 200 000	8.98 ± 0.03	5.12 ± 0.04	0.398 ± 0.002

†Average values up to 100 kHz.
‡Not dependent on angle because their positions relative to the source are the same and correlation is mainly from single particles from the source.
§Depends on angle because of asymmetry of emission of multiple neutrons from the same source fission.

threshold without changing the physical size of the detectors and because the measured value of $R(\omega)$ is available for comparison purposes. The calculations were performed for neutrons since the ratio of spectral densities from the gamma-ray response is calculated with the same routines that are used to calculate the ratio of spectral densities with the neutron response.

To demonstrate that the ratio of spectral densities is independent of the source size, the number of source disintegrations per data block was varied. This corresponds to varying the intensity of the ^{252}Cf source. The results of these calculations are given in Table 3, and indicate that the ratio of spectral densities is indeed independent of the source strength as verified by measurements with uranium systems. To demonstrate that the ratio of spectral densities is independent of the detector efficiency, several calculations were performed by varying the neutron threshold of the detector. By increasing the neutron threshold, the number of neutrons that contribute to the detector response is reduced while the reflection effects of the detector on the neutron multiplication factor do not change. Table 3 also contains a comparison of the results obtained from these calculations. From these analyses, it is obvious that the calculated ratio of spectral densities behaves in the same manner as the measured values, independent of source intensity for this case.

3. COMPARISON OF MEASURED AND CALCULATED FREQUENCY ANALYSIS PARAMETERS FOR URANIUM METAL CYLINDERS

3.1. Uranium metal cylinders

An unmoderated, unreflected uranium metal system (Mihalczo, 1964; Mihalczo *et al.*, 1987) was analyzed to determine the ability of the code to calculate the gamma ray response. The experimental configuration for these measurements consisted of several 177.71-mm diameter right-circular cylinders. The cylinders were supported by a 0.25-mm thick stainless steel diaphragm held in position by an aluminum clamping ring. This structure supported the cylinder 2.7 m above the floor and was positioned 3 m away from the nearest wall. A sketch of the model of the experimental set-up is provided in Fig. 8. The uranium metal cylinders have been described previously in this article. In the measurements, the ^{252}Cf source was located at the center top surface of the cylinders. The ^{6}Li-glass scintillators were positioned at the midplane of the cylinders, placed 180° apart

Table 3. Calculation of ratio of spectral densities for 292-mm high uranyl nitrate solution system for varying source intensity and detection efficiency

Number of data blocks	^{252}Cf source strength (fissions/block)	Neutron threshold†	$R(\omega)$
5000	32	0.8 MeV	0.0446 ± 0.0006
10000	32	1.5 MeV	0.0451 ± 0.0006
25000	16	0.8 MeV	0.0451 ± 0.0003

†Variation in the neutron detector efficiency obtained by variation of the threshold.

and adjacent to the radial surface. These detectors had a diameter of 38.1 mm and were 25.4 mm long. Lithium-6–glass scintillators are sensitive to both neutrons and gamma rays. Since the energy distribution of neutrons in these cylinders is a slightly degraded fission emission spectrum, much of the detector response is from gamma rays. Most of the neutron response is in the energy range around 300 keV, where ^{6}Li has a large neutron resonance cross-section.

The calculation model for this system consisted of a uranium metal cylinder with the detectors and the source. Measurements with these uranium metal cylinders were first performed in 1975 and were repeated in 1984 with different detectors and different sources. The ratios of spectral densities from both sets of measurement were in good agreement and demonstrated that the measurements are reproducible. Calculations were performed for four different cylinder heights using ENDF/B-IV (Garber, 1975) cross-sections to compare with results obtained from KENO-NR calculations. Table 4 is a comparison of the low-frequency values of $R(\omega)$ obtained from the measurement, the KENO-NR calculations (Ficaro, 1991) and the MCNP-DSP calculations. The low-frequency values of $R(\omega)$ from the MCNP-DSP calculations are for the combined neutron and gamma-ray responses, while the low-frequency values of $R(\omega)$ from the KENO-NR calculations are only from neutrons, since KENO-NR is a neutron-only Monte Carlo code. For these four cylinder heights, there is excellent agreement between both calculation and the measurement. This demonstrates that the MCNP-DSP calculation achieves results

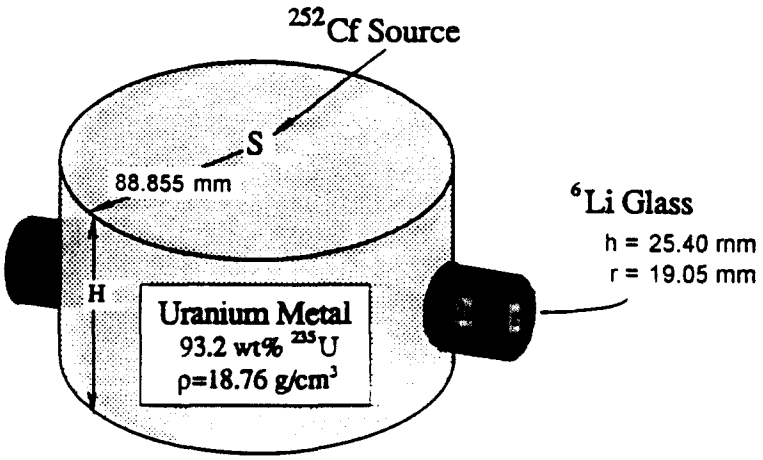

Fig. 8. Source–detector configuration for uranium metal cylinders of varying height.

Table 4. Comparison of ENDF/B-IV calculations of $R(\omega)$ for uranium metal cylinders with measurements

Cylinder height (mm)	KENO-NR	MCNP-DSP	Measurements
101.6	0.0697 ± 0.0041	0.0695 ± 0.0003	0.0694 ± 0.0008
91.4	0.101 ± 0.009	0.108 ± 0.001	0.0995 ± 0.0013
81.3	0.160 ± 0.012	0.156 ± 0.001	0.150 ± 0.003
71.1	0.215 ± 0.015	0.214 ± 0.002	0.215 ± 0.006

similar to those of KENO-NR and sufficiently reproduces the measured values for the unmoderated, unreflected uranium metal cylinders. A comparison of the frequency dependences of $R(\omega)$ is not possible because of the limited frequency response of the measurement system used in this experiment.

MCNP-DSP calculates the detector responses to neutrons and gamma rays. The neutron and gamma-ray responses can also be combined to form the total detector response. Table 5 is a comparison of the low-frequency values of $R(\omega)$ obtained from the neutron, gamma ray, and combined neutron and gamma ray responses using the ENDF/B-IV cross-section data sets. For the average values of $R(\omega)$ there is good agreement between the neutron, gamma ray, and combined neutron and gamma ray responses. The frequency dependence of the various spectral densities is also in good agreement. Various APSDs, CPSDs, and coherences are plotted as a function of frequency in Figs 9–14 for the 91.4-mm high uranium metal cylinder. The spectra are normalized to their low-frequency values. Figure 9 is a plot of the normalized APSD G_{22} as a function of frequency for the neutron and gamma ray responses. These APSDs have essentially the same frequency dependence. Differences at the high frequencies are less than 1%. Figures 10 and 11 show the frequency dependence of the normalized CPSDs, G_{12}, and G_{23}. The frequency dependence of the CPSDs are also in good agreement. The normalized coherences are plotted in Figs 12 and 13. The frequency dependence of coherences are in good agreement. Finally, Fig. 14 is a plot of the normalized value of $R(\omega)$. These frequency spectra demonstrate that the detector responses in this case are independent of the particle that causes the detection since gamma rays from fission can also be used to obtain correlated information about the fission chain multiplication process.

The ratio of spectral densities obtained from the gamma-ray response agrees well with that obtained from the neutron response. This is expected because gamma rays from fission represent the fluctuations in the fission chain multiplication process as well as neutrons. The difference between the measured low-frequency value of $R(\omega)$ and the

Table 5. ENDF/B-IV calculated values of $R(\omega)$ and k_{eff} as a function of height for uranium metal cylinders with source at top and with ^{6}Li-glass detectors

Cylinder height (mm)	$R(\omega)$ (neutron)	$R(\omega)$ (photon)	$R(\omega)$ (neutron and photon)	k_{eff}
101.6	0.0712 ± 0.0008	0.0704 ± 0.0005	0.0695 ± 0.0003	0.9268 ± 0.0004
91.4	0.109 ± 0.001	0.105 ± 0.001	0.108 ± 0.001	0.8879 ± 0.0005
81.3	0.165 ± 0.003	0.151 ± 0.001	0.156 ± 0.001	0.8424 ± 0.0004
71.1	0.216 ± 0.004	0.210 ± 0.003	0.214 ± 0.002	0.7903 ± 0.0004

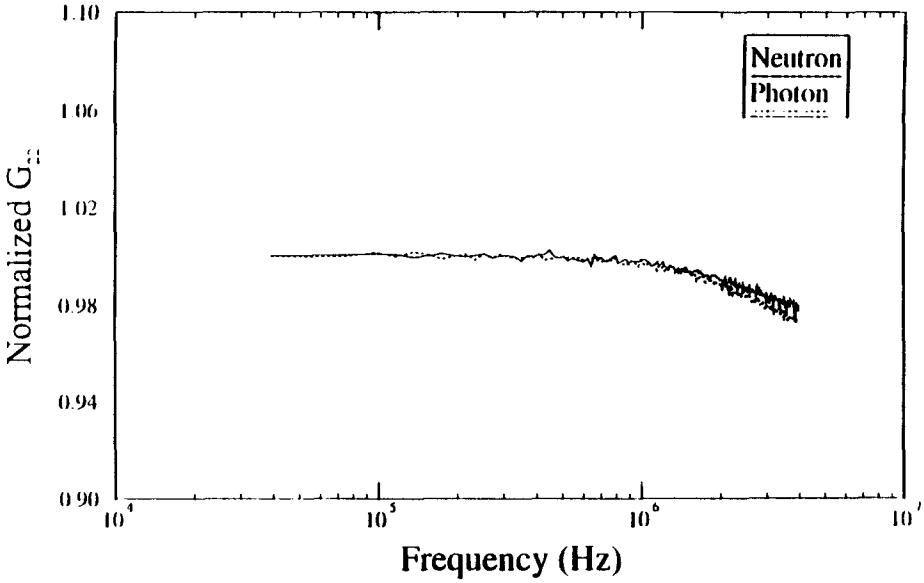

Fig. 9. Comparison of the calculated normalized G_{22} from the neutron and gamma ray response for the 91.4-mm-high uranium metal cylinder.

calculated low-frequency value of $R(\omega)$ from the gamma-ray response varies from 2 to 9%. The most significant result from these calculations is that the low-frequency value of $R(\omega)$ from the gamma-ray response agrees well with that obtained from the neutron response.

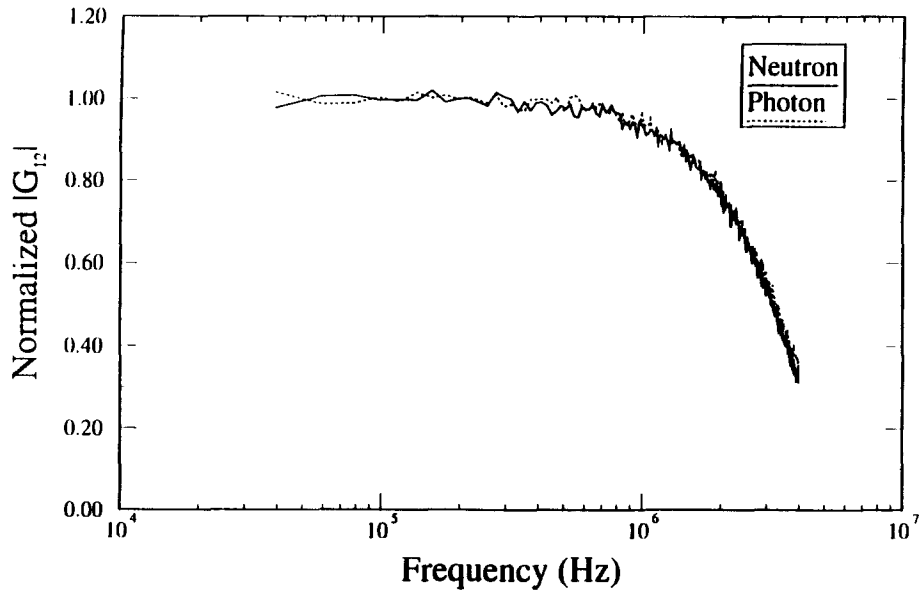

Fig. 10. Comparison of the calculated normalized G_{12} from the neutron and gamma ray response for the 91.4-mm-high uranium metal cylinder.

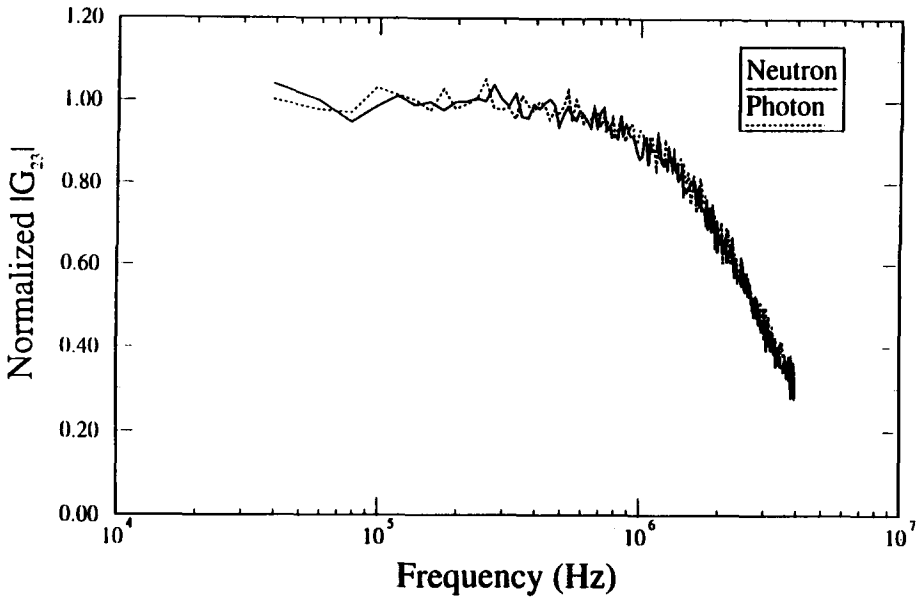

Fig. 11. Comparison of the calculated normalized G_{23} from the neutron and gamma ray response for the 91.4-mm-high uranium metal cylinder.

The results of calculations for different cylinder heights employing the ENDF/B-V cross-sections (Kinsey, 1979) are presented in Table 6. The low-frequency values of $R(\omega)$ and the values of k_{eff} from measurements are presented in Table 7. The difference between the calculated and measured values of $R(\omega)$ varies from 2 to 15%. However, the

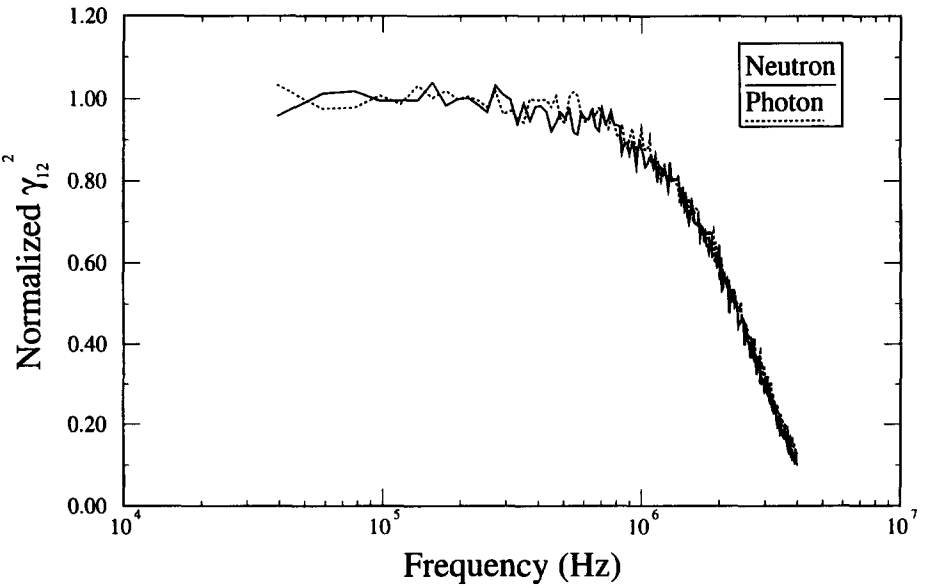

Fig. 12. Comparison of the calculated normalized γ_{12}^2 from the neutron and gamma ray response for the 91.4-mm-high uranium metal cylinder.

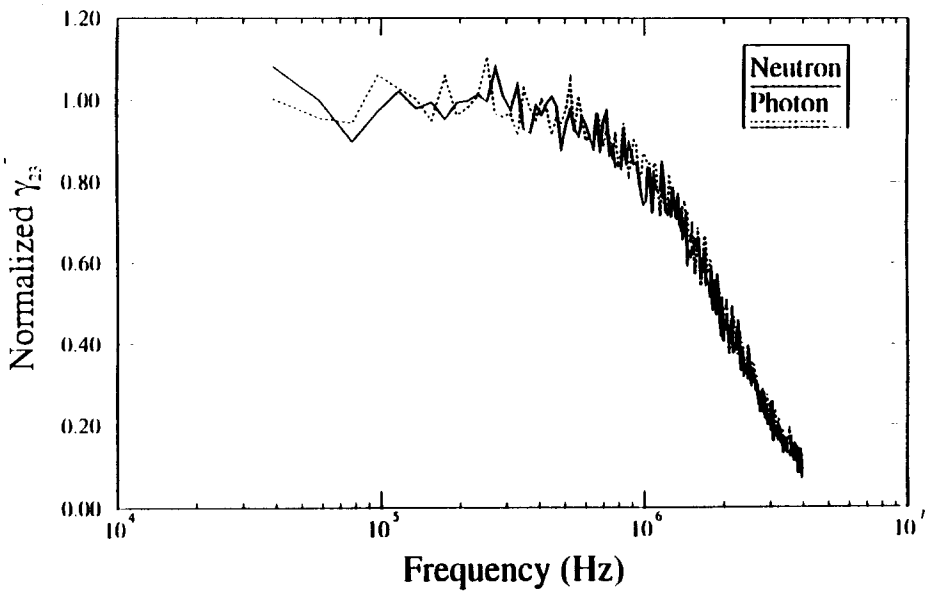

Fig. 13. Comparison of the calculated normalized γ_{23}^2 from the neutron and gamma ray response for the 91.4-mm-high uranium metal cylinder.

calculated values of k_{eff} are consistently lower than the measured values of k_{eff}, as can be seen from the results presented in Tables 6 and 7. Because the calculated values of k_{eff} are lower than the measured values of k_{eff}, the calculated low-frequency value of $R(\omega)$ should be greater than the measured value. This behavior is evident in Table 6. Because the

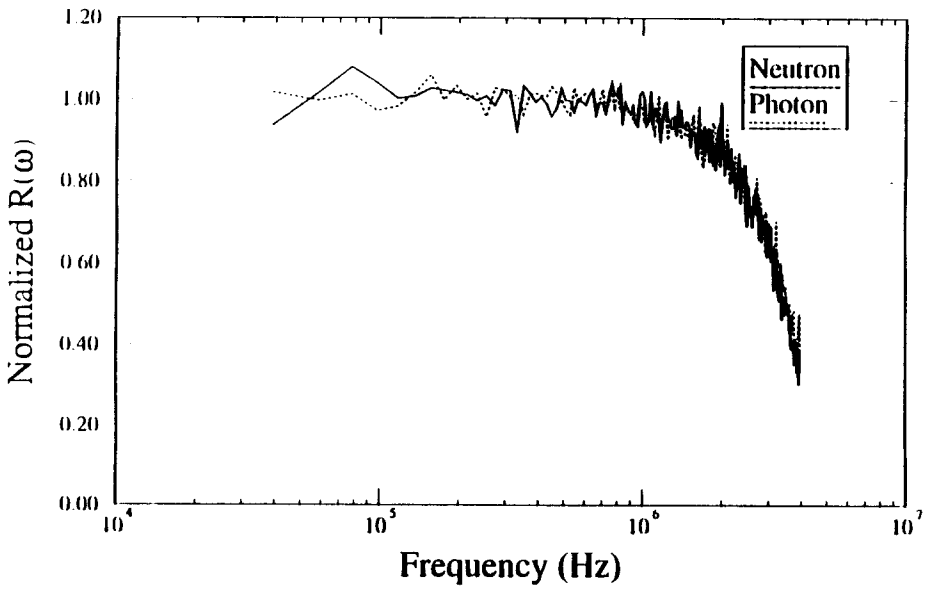

Fig. 14. Comparison of the calculated normalized $R(\omega)$ from the neutron and gamma ray response for the 91.4-mm-high uranium metal cylinder.

Table 6. ENDF/B-V calculated values of $R(\omega)$ and k_{eff} as a function of height for uranium metal cylinders with source at top and with ^{6}Li-glass detectors

Cylinder height (mm)	$R(\omega)$ (neutron)	$R(\omega)$ (photon)	$R(\omega)$ (neutron and photon)	k_{eff}
101.6	0.0736 ± 0.0005	0.0711 ± 0.0003	0.0715 ± 0.0002	0.9193 ± 0.0004
91.4	0.1129 ± 0.0007	0.1116 ± 0.0005	0.1120 ± 0.0004	0.8806 ± 0.0005
81.3	0.178 ± 0.0025	0.1631 ± 0.0012	0.1632 ± 0.0009	08361 ± 0.0004
71.1	0.237 ± 0.005	0.225 ± 0.002	0.223 ± 0.002	0.7834 ± 0.0004
61.0	0.3184 ± 0.0077	0.2839 ± 0.0088	0.2815 ± 0.0052	0.7227 ± 0.0004

Table 7. Measured values of $R(\omega)$ and k_{eff} as a function of height for uranium metal cylinders with source at top and with ^{6}Li-glass detectors

Cylinder height (mm)	$R(\omega)$	k_{eff}
101.6	0.0694 ± 0.0008	0.929 ± 0.001
91.4	0.0995 ± 0.0013	0.904 ± 0.001
81.3	0.150 ± 0.003	0.859 ± 0.003
71.1	0.215 ± 0.006	0.799 ± 0.007
61.0	0.298 ± 0.018	0.717 ± 0.020

ratio of spectral densities is a function of k_{eff}, a small difference in the k_{eff} values results in a larger difference in the values of $R(\omega)$, which is also evident from the results presented in Table 6. The discrepancies between the calculations and the measurements in these unmoderated, unreflected uranium metal cylinders may be due to small discrepancies in the cross-sections or other nuclear data that could result in errors in the calculated values of $R(\omega)$ and k_{eff}.

A calculation was also performed for the 101.6-mm high uranium metal cylinder using ENDF/B-VI cross-sections (Rose, 1991). A comparison of the results of the calculations for the 101.6-mm high uranium metal cylinder using the ENDF/B-IV, ENDF/B-V, and ENDF/B-VI (Kinsey, 1979) cross-sections is presented in Table 8. As can be seen from these results, the best agreement is obtained with the ENDF/B-IV cross-section data set. The results of the ENDF/B-VI calculation show a large disagreement with the measured values of $R(\omega)$. The calculated value of k_{eff} using the ENDF/B-VI is 1.0% lower than the measured value of k_{eff}. This reduction in k_{eff} results in the ratio of spectral densities being overpredicted by 11.0%. It is beyond the scope of this work to define what inadequacy in the cross-section data produced these differences.

3.2. Tightly coupled uranium metal cylinders

To further demonstrate the ability to obtain the ratio of spectral densities from the gamma-ray response only, a uranium metal system separated by borated plaster using NaI detectors, which are sensitive only to gamma rays, was analyzed. The uranium metal cylinders are the same materials as those just described. The uranium metal cylinders

Table 8. Effects of cross section data on calculated values of $R(\omega)$ and k_{eff} for 101.6-mm-high uranium metal cylinder†

Cross data set	Number of data blocks	$R(\omega)$ (neutron)	$R(\omega)$ (photon)	$R(\omega)$ (neutron and photon)	K_{eff}
ENDF/B-IV	71 000	0.0712 ± 0.0008	0.0704 ± 0.0005	0.0695 ± 0.0003	0.9268 ± 0.0004
ENDF/B-V	64 000	0.0736 ± 0.0005	0.0711 ± 0.0003	0.0715 ± 0.0002	0.9193 ± 0.0004
ENDF/B-VI	44 000	0.0771 ± 0.0011	0.0747 ± 0.0009	0.0758 ± 0.0007	0.9178 ± 0.0004

†Measured: $R(\omega) = 0.0694 \pm 0.0008$; $k_{eff} = 0.929 \pm 0.001$.
KENO-NR with ENDF/B-IV cross-sections: $R(\omega) = 0.0697 \pm 0.0004$; $k_{eff} = 0.927 \pm 0.002$.

were 50.8 mm high with a 177.71 mm ID. These coupled cylinders were separated by a 10.2-mm high, 177.71-mm ID borated plaster disk. The NaI detectors were positioned 180° apart, 6.35 mm away from the radial surface of the second cylinder and were contained in a 12.9-mm thick lead cup to shield the detectors from the natural emission of gamma rays from uranium. A sketch of this configuration is shown in Fig. 15.

Only one measurement was calculated with this configuration. The measured low-frequency value of $R(\omega)$ is 0.102 ± 0.003 for 11 000 blocks of data. Since only the low-frequency value of $R(\omega)$ was available experimentally, a comparison of the frequency dependences of $R(\omega)$ could not be made. The measured value of k_{eff} obtained from the low-frequency value of $R(\omega)$ is 0.900 ± 0.003. The calculations were performed with the ENDF/B-V cross-sections since improved gamma production data are available in the ENDF/B-V data. The calculated low-frequency value of $R(\omega)$ is 0.109 ± 0.003 for 160 000 blocks of data. The calculated value of k_{eff} is 0.886 ± 0.001. The difference between the measured and calculated low-frequency values of $R(\omega)$ is consistent with the results previously presented for uranium metal cylinders and is consistent with the lower calculated values of the k_{eff}. These results further indicate that the ratio of spectral densities can be calculated using either the neutron or the gamma ray response.

4. CONCLUSIONS

A series of calculations were performed to validate the MCNP-DSP code. To validate the ^{252}Cf neutron and gamma-ray energy spectra and the detection process, a calculation was performed with the source and detector separated by 1.1 m in air. The calculated neutron response as a function of time after ^{252}Cf fission agreed well with the measured neutron response for this source and detector configuration. The calculated gamma-ray response differed from the measured gamma-ray response because the measured gamma-ray response included the time resolution of the measurement system, causing the gamma peak to be spread out over time. However, the integrals of the peaks are in good agreement, and thus the calculated gamma-ray time distribution is considered to be in good

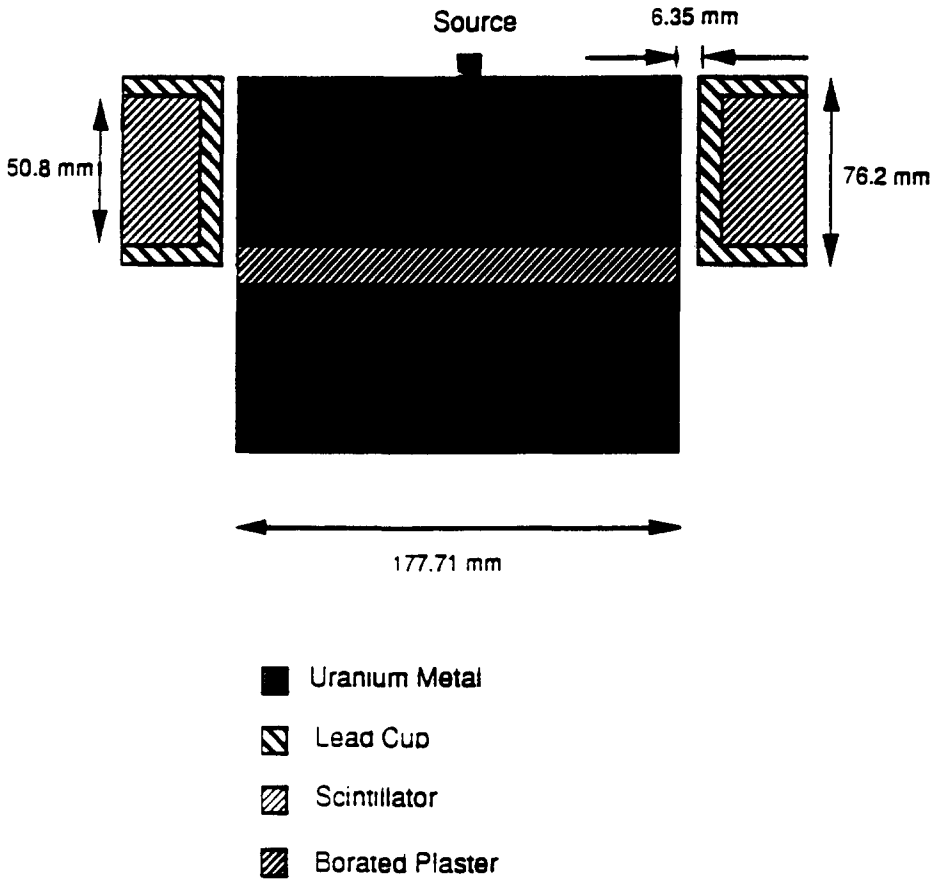

Fig. 15. Coupled uranium metal cylinder configuration.

agreement with the measured distribution. To show that the code placed the detected events at the proper time, a calculation was performed with a piece of beryllium placed between the source and detector separated by 1 m in air. The depression in the neutron response occurred at a time that is directly related to a known 2.78 MeV resonance in the beryllium cross-section. To validate the Fourier processing algorithms, two calculations were performed with the source placed between two adjacent detectors. Excellent agreement between the calculated value of $R(\omega)$ and the theoretically exact value of $R(\omega)$, which is obtained from the emission probability distribution, was obtained for both the neutron and gamma-ray responses. Next, a series of calculations was performed to demonstrate that the frequency spectra are not dependent on the manner in which the spectra are calculated. There was excellent agreement between the frequency spectra obtained by direct Fourier transforming the blocks of data obtained from detector responses and by Fourier transforming the correlation functions. In addition, it was demonstrated that the convergence of the calculations is the same. This validates the calculation of the frequency spectra and correlation functions. The value of $R(\omega)$ obtained from the calculations has been shown to be independent of the source strength and the detection efficiency, as had been established in the measurements.

Several calculations were performed for the systems measured. Using the ENDF/B-IV cross-sections, good agreement was obtained between the calculated and measured values of $R(\omega)$. These results also showed that in this case the frequency spectra obtained from the neutron and gamma-ray responses have the same frequency dependence. This was expected since the gamma rays from fission can be correlated in a manner similar to that in which neutrons from fission are correlated. The significant result from these calculations is that the calculated low-frequency value of $R(\omega)$ obtained from the gamma-ray response agrees well with that obtained from the neutron response and that the neutron and gamma ray spectra have the same frequency dependence.

Thus, MCNP-DSP provides a more general continuous-energy Monte Carlo model for the calculation of measured observables that includes not only neutrons but also gamma rays. This code can be used to calculate frequency analysis parameters for relevant in-plant configurations of fissile material. Agreement with the measured data for a particular application will verify the calculation and hence the calculated value of k_{eff} for the particular application. MCNP-DSP can be used to validate calculational methods and cross-section data sets with measured data from subcritical experiments. In most cases the frequency analysis parameters are more sensitive to cross-section changes by as much as 1 or 2 orders of magnitude and thus may be more useful than comparisons of neutron multiplication factors for calculational validation. The use of the MCNP-DSP model in place of a point kinetics model to interpret subcritical experiments extends the usefulness of this measurement method to systems with much lower neutron multiplication factors. MCNP-DSP can also be used to determine the calculational bias in the neutron multiplication factor (a quantity that is essential to the criticality safety specialist) from in-plant subcritical experiments. MCNP-DSP provides a more general tool for planning experiments for criticality safety, safeguards, nondestructive assay, and arms control verification.

REFERENCES

Brunson, G. S. Jr (1982) Multiplicity and Correlated Energy of Gamma Rays Emitted in the Spontaneous Fission of Californium-252. PhD Thesis, University of Utah.

Ficaro, E. P. (1991) KENO-NR: A Monte Carlo Code Simulating the ^{252}Cf-Source-Driven Noise Analysis Experimental Method for Determining Subscriticality. PhD Dissertation, University of Michigan.

Garber, D. (1975) *ENDF-201, ENDF/B Summary Documentation.* BNL-17541, Brookhaven National Laboratory.

Kinsey, R. (1979) *Data Formats and Procedures for the Evaluated Nuclear Data File, ENDF.* Brookhaven National Laboratory Report, BNL-NCS-S0496 (ENDF 102) 2nd edn (ENDF/B-V).

Mihalczo, J. T. (1964) *Nucl. Sci. Engng* **20**, 60.

Mihalczo, J. T. (1970) *Nucl. Sci. Engng* **41**, 296.

Mihalczo, J. T. (1971) *Nucl. Sci. Engng* **46**, 147.

Mihalczo, J. T. and Hill, N. W. (1971) *Trans. Am. Nucl. Soc.* **14**, 60.

Mihalczo, J. T., King, W. T. and Blakeman, E. D. (1987) *Nucl. Sci. Engng* **95**, 1.

Mihalczo, J. T., Blakeman, E. D., Ragan, G. E., Johnson, E. B. and Hachiya, Y. (1990) *Nucl. Sci. Engng* **104**, 314.

Paré, V. K. and Mihalczo, J. T. (1975) *Nucl. Sci. Engng* **56**, 213.

Rose, P. F. (1991) *ENDF-201, ENDF/B–VI Summary Documentation.* BNL-17541, Brookhaven National Laboratory.

Spencer, R. R., Gwin, R. and Ingle, R. (1982) *Nucl. Sci. Engng* **80**, 603.
Valentine, T. E. and Mihalczo, J. T. (1996) MCNP-DSP: A Neutron and Gamma Ray Monte Carlo Calculation of Source-Driven Noise-Measured Parameters *Ann. Nucl. Energy*.